J.Natn.Sci.Foundation Sri Lanka 2025 53 (3): 245 - 258
DOI: http://dx.doi.org/10.4038/jnsfsr.v53i3.12649

RESEARCH ARTICLE

Biological Imaging

Visualizing changes in internal layers of Chinese chives leaf under short-term ozone exposure with biospeckle optical coherence tomography

LKT Srimal[1,5*], UM Rajagopalan[2], H Kadono[3] and T Yonekura[4]
[1] *Department of the Mechanical and Manufacturing Engineering, Faculty of Engineering, University of Ruhuna, Sri Lanka.*
[2] *Department of Mechanical Engineering, Shibaura Institute of Technology, 3-7-5 Toyosu, Koto City, Tokyo, 135-8548, Japan.*
[3] *Graduate School of Science and Engineering, Saitama University, 255 Shimo-okubo, Sakura-ku, Saitama-shi, Saitama, 338-8570, Japan.*
[4] *Center for Environmental Science in Saitama, Kazo, Saitama 347-0115, Japan.*
[5] *Department of Mechanical Engineering, Faculty of Engineering, South Eastern University of Sri Lanka, Oluvil, Sri Lanka.*

Submitted: 24 April 2025; Revised: 22 August 2025; Accepted: 27 August 2025

Abstract: Ozone (O_3) stress can cause physiological changes as well as changes in the growth patterns of plants. Conventional techniques for studying these changes in plants require destruction of the sample and a subsequent analysis, thus the plant's responses to external stress are inferred indirectly. In this paper, we show that a biospeckle optical coherence tomography (bOCT) biospeckle imaging can be used to monitor the response of Chinese chives leaves to O_3 stress. A Fourier-domain OCT operating at a wavelength of 836 nm with a depth of resolution of 6 µm was used. The bOCT biospeckle image was obtained by calculating the standard deviation of the OCT signal along the time axis at each point of the selected portion of the cross-sectional image from the successively acquired OCT images. In the bOCT biospeckle images, the internal layer structure could be clearly visualized, especially the mesophyll cells with high contrast in comparison to the structural OCT image. In addition, an analysis of the average autocorrelation functions of the biospeckle signals revealed that the correlation length decreased in the mesophyll layer during O_3 exposure, possibly indicating the increase in movements of internal structures within the leaf. Our results suggest that biospeckle imaging can be a suitable technique for fast and non-destructive monitoring of environmental stresses on plants, in contrast to conventional techniques that require a few days' to a few weeks' time, with destruction followed by subsequent analysis, thus paving the way for significant time saving.

Keywords: Biological activities, biospeckles, correlation length, biospeckle optical coherence tomography (bOCT), ozone, temporal characteristics.

INTRODUCTION

Surface (tropospheric) ozone (O_3) is a secondary air pollutant, generated by a series of reactions involving oxides of nitrogen (NOx) and volatile organic compounds (VOCs) in the presence of UV radiation from sunlight (Darrall, 1989; Ashmore, 2005; Ainsworth, 2008; Kumar *et al.*, 2021; Santiago *et al.*, 2022; Yoshikado, 2023). Its disastrous effect is spreading over an enormous land area of world, especially in industrialized countries such as China, India, and even in Japan (Kobayashi *et al.*, 1995; Kobayashi & Okada, 1995; Beig *et al.*, 2007; Wang *et al.*, 2007; Lee & Goto, 2022; Santiago *et al.*, 2022; Wang *et al.*, 2022; Wei *et al.*, 2022, Yoshikado, 2023). The O_3 contaminated environment causes a wide range of effects including visible leaf injury, and growth and yield reductions in both agricultural crops and forest trees (Kobayashi & Okada, 1995; Wang *et al.*, 2007; Jiménez-Montenegro *et al.*, 2021; Feng *et al.*, 2021; Holder & Hayes, 2022; Panebianco *et al.*, 2022). Conventional techniques such as microscopic observation, and chemical analysis are commonly performed to monitor the effect of O_3 on plants for their structural changes (Calatayud *et al.*, 2003). However, these conventional techniques cannot be performed non-destructively in real-time and *in vivo*. Moreover, it is important to observe the internal structure of a plant leaf when it is under an environmental stress.

* Corresponding author (srimal@mme.ruh.ac.lk; https://orcid.org/0000-0002-3285-3214)

This article is published under the Creative Commons CC-BY-ND License (http://creativecommons.org/licenses/by-nd/4.0/). This license permits use, distribution and reproduction, commercial and non-commercial, provided that the original work is properly cited and is not changed in anyway.

Recently, a non-invasive interferometric technique, statistical interferometry, that is capable of measuring fast and accurate measurement of growth changes under environmental stresses such as O_3 has been demonstrated *in vivo* (Rathnayake *et al.*, 2008; Kobayashi & Kadono, 2010; Thilakarathne *et al.*, 2014a, 2014b; DeSilva *et al.*, 2017). However, this measurement is limited to a small area of a sample. Here we consider an optical technique called optical coherence tomography (OCT) that has the potential for making a volumetric measurement at high speed and at micrometer resolutions (Huang *et al.*, 1991; Fercher, 1996; Fujimoto, 2003; Regar *et al.*, 2007; Srimal, 2015; Ge *et al.*, 2021; Saleah *et al.*, 2021; Saleah *et al.*, 2022; Saleah *et al.*, 2023).

The OCT technique is based on interferometric detection of a low coherent light backscattered from a sample and can provide non-contact two or three dimensional *in vivo* tomographic images of internal tissue structure. Since depth resolution of OCT is limited by the coherence length of the light source, a relatively high resolution of the order of a few micrometers can be achieved (Fujimoto & Drexler, 2008; Lee *et al.*, 2018; Zheng *et al.*, 2021; Bouma *et al.*, 2022). OCT is being widely employed for the visualization of the internal structure of tissues (Wijesinghe *et al.*, 2016a; Ravichandran *et al.*, 2017). Many pathological processes, such as dysplasia and cancer, alter the layered structure of healthy tissue and these changes can be detected by OCT (Steiner *et al.*, 2003; Gladkova *et al.*, 2008; Fercher, 2010; Lee *et al.*, 2018; Rajagopalan *et al.*, 2020; Li *et al.*, 2021b). On the other hand, it is widely used in the field of ophthalmology (Wijesinghe *et al.*, 2016b; Everett *et al.*, 2021; Wei & Gu, 2021; Micieli *et al.*, 2021; Drexler *et al.*, 2001; Wojtkowski *et al.*, 2002; Pircher *et al.*, 2011; Srinivasan *et al.*, 2009). Due to its high resolution, OCT technique for imaging plants (Hettinger *et al.*, 2000; Reeves *et al.*, 2002; Boccara *et al.*, 2007; Srimal, 2015; de Wit *et al.*, 2020; Beiu *et al.*, 2022; Li *et al.*, 2022) has been getting attention. Non-invasive visual inspection of plant leaf *in vivo* may be useful for evaluating the physiological state of plants under the influence of environmental stresses such as O_3, acid mine drainage (Li *et al.*, 2021a), effect of nanoparticles (De Silva *et al.*, 2023a), effect of heavy metals (De Silva *et al.*, 2021), and the effect of micro particles of plastics (De Silva *et al.*, 2022, 2023b).

The potential of OCT in monitoring such biological activities in human and animal organelles has been demonstrated, in the visual cortex of animal brains (Maheswari *et al.*, 2002, 2003; Khateeb *et al.*, 2022) and rat somatosensory cortex (Chen *et al.*, 2009; Hope *et al.*, 2021) and retina (Moayed *et al.*, 2011; Kashani *et al.*, 2021). We propose to monitor physiological changes in plants under environmental stress (O_3) by OCT (Srimal *et al.*, 2013, 2015; Lichtenegger *et al.*, 2020)

In OCT images, speckles are considered as a noise and are usually temporally averaged (Szkulmowski *et al.*, 2012; Silva *et al.*, 2022). In this study, we focused on the temporal characteristics of speckles, as those could indicate the dynamic activities within the tissues, also called biospeckles (Asakura, 1996; Tang *et al.*, 2021a, 2021b; Aizu &). When coherent laser light illuminates a sample under investigation, the backscattered light randomly interferes, and a speckle pattern is generated at a certain observation plane. If the investigating sample and the scatterers inside the sample are not moving, then the speckle pattern is also stationary. However, when the sample or the scatterers are moving as in biological tissues, the speckle pattern changes randomly resulting in biospeckles. In plants, such dynamic processes could be attributed to factors such as cytoplasmic streaming, organelle movement, cell growth and division, and biochemical reactions (Mogre *et al.*, 2020; Mathur, 2020; Braga *et al.*, 2009). Thus, the biospeckles can reflect the activities of biological tissue (Kurenda *et al.*, 2012; Ansari & Nirala, 2013; Zdunek *et al.*, 2014; Rajagopalan *et al.*, 2020; Li *et al.*, 2021a).

Especially, in agriculture, the analysis of seeds (Braga *et al.*, 2003; Li *et al.*, 2021a), the identification of plant diseases (Ravichandran *et al.*, 2016), leaf quality assessment (Wijesinghe *et al.*, 2016a, 2017b), detection of germination rate (Wijesinghe *et al.*, 2017a), the analysis of fungi (Braga Jr *et al.*, 2005; Singh *et al.*, 2021), monitoring of maturation and diseases in fruits (Pajuelo *et al.*, 2003; Wijesinghe *et al.*, 2018), observation of root growth (Braga *et al.*, 2009; De Silva *et al.*, 2023a, 2023b), and evaluation of animal semen (Carvalho *et al.*, 2009) were performed. In medicine, we can find applications in the study of the brain, skin and blood flow (Fujii *et al.*, 1985; Li *et al.*, 2006). A few reports exist on the application of OCT speckles in the observation of biological tissues (Mariampillai *et al.*, 2008, 2010; Baum *et al.*, 2020).

In this study, we propose a Biospeckle Optical Coherence Tomography (bOCT) based on biospeckle to study the effect of environmental stresses on plants in a short period of time which is not possible with other conventional methods (Srimal *et al.*, 2014; Srimal, 2015). Here, we examined the immediate response of leaves of *Allium tuberosom* commonly known as Chinese chives to short-term exposure of O_3, by analyzing the bOCT biospeckle signals coming from various depths. Mesophyll cell layers, and the immediate responses are better visualized using the bOCT images rather traditional OCT images.

MATERIALS AND METHODS

Optical system

A schematic of our spectral domain OCT (SD-OCT) system is shown in Figure 1. The light source is a super-luminescent diode (SLD) centred at wavelength 836.1 nm and having a bandwidth of 55.2 nm. A 99:1 optical fiber coupler was used to split the light into the sample and reference arms of the fiber-optic interferometer. Light reflected from the sample was combined with the light reflected from the reference mirror M1. The axial and lateral resolutions of the OCT system were estimated to be 6 μm and 22 μm, respectively. Identical lenses, L3 and L4, were placed in the sample and reference arms to cancel dispersion mismatch between the two arms. Collimating the output beam from the optical fiber of the circulator using lens, L5, the spectral interference signal was obtained by using grating, lens L6, and line-scan camera. We used line scan CCD camera (L104k-2k, BASLER, Germany) with 2048 pixels.

(a)
(b)

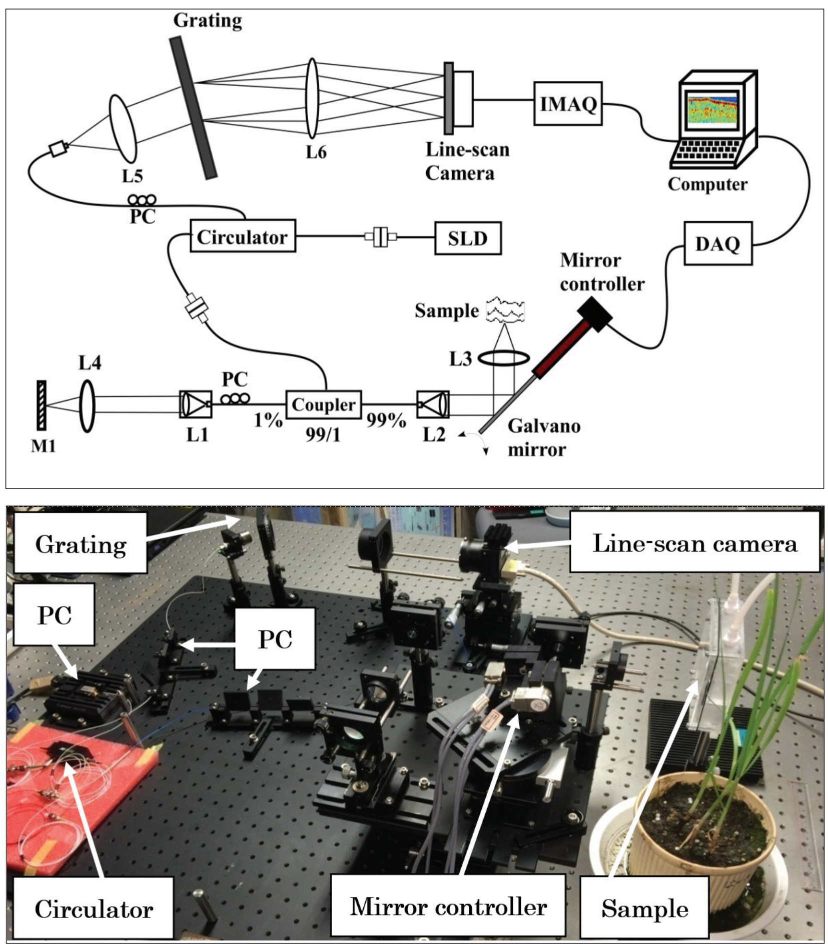

Figure 1: (a) A sketch, and (b) Photograph of, experimental setup of spectral domain optical coherence tomography system. SLD: super luminescent diode, L1~L6: lenses, M1: mirror, PC: polarization controller, DAQ: data acquisition device, IMAQ: image grabber.

A software application (using LabVIEW 2011, National Instruments, USA) was developed to realize the OCT system utilizing the biospeckle signals from a target area of the sample. Driving voltages for galvano mirrors were applied through a D/A converter of the data acquisition device (DAQ, PCIe-1429, National Instruments, USA) to laterally scan the beam across the sample surface. The imaging data from the line scan camera was acquired by an image grabber (IMAQ, PCIe-6351, National Instruments, USA).

Autocorrelation function of the biospeckle signal

While the scanning mechanism was being stopped at a lateral position of interest, the spectral interference signals were acquired with a sampling frequency of 25,000 lines/sec for1.2 seconds. The acquired spectral interference signal $I(\lambda, t)$ from the camera at time, t, was first converted into the signal $I(k, t)$ in wave number, k, space from wavelength, λ, space as given by,

$$I(k,t) = I(2\pi/\lambda, t). \quad ...(1)$$

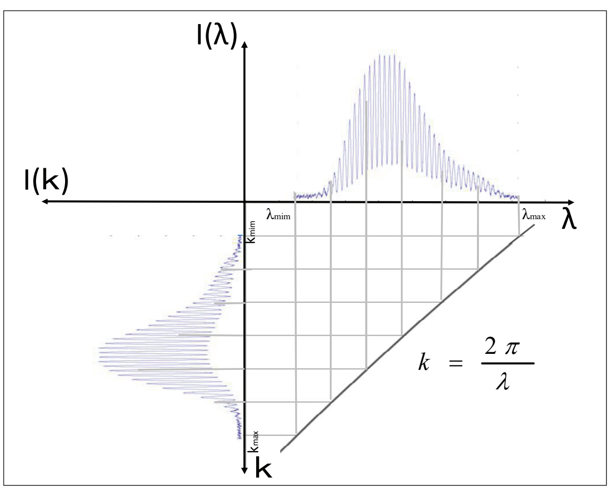

Figure 2: Transformation of signal in wavelength (λ) space to wave number (k) space (rescaling).

Next, the rescaled signal of $I(k,t)$ was Fourier transformed in order to obtain the depth resolved reflectivity profile $r(d,t)$ of the sample along the sample beam as,

$$r(d,t) = \int_{-\infty}^{\infty} I(k,t)\, exp(-2\pi ikd)dk, \quad ...(2)$$

where d is the depth of the sample. Finally, a total of 25000×1.2 depth resolved reflectivity profiles were obtained. They were stored in the computer memory as a two-dimensional data array representing the variation along time, and we call this as time history OCT image. The rows and columns of the data array represent the depth positions, and their intensities in a sequence of regularly spaced time steps of 1/25,000 seconds, respectively.

The biological activity of the sample could be reflected in the temporal characteristics of intensity changes in the horizontal direction, that is, along the rows. Therefore, we utilized the autocorrelation function and its correlation length to evaluate the biological activities of the tissue.

By repeating the data acquisition 5 times, five-time history OCT images were acquired over 6 seconds. Power spectral densities $|R(d,f)|^2$ of time signals express by equation (2) were calculated at every depth position along the time axis. Here, f denotes temporal frequency. To get a higher signal to noise ratio (SNR), five power spectral densities corresponding to each depth position were averaged across the time history OCT images. Finally, averaged power spectral densities $\langle|R(d,f)|^2\rangle$ were inverse Fourier transformed to get the autocorrelation functions $\Gamma(d,\tau)$ at a certain depth position, d, as given by,

$$\Gamma(d,\tau) = \int_{-\infty}^{\infty} \langle|R(d,f)|^2\rangle\, exp(2\pi f\tau)\, df \quad ...(3)$$

We used the software, MATLAB (MATLAB2009a, MathWorks, USA) for calculations of the autocorrelation function. The temporal variations of biospeckles were quantified by calculating the correlation length (CL) which is half width half maximum of the autocorrelation function. This quantity was employed as a measure for the biological activities of layers at different depths of the Chinese chives leaf under O_3 stress. When the signal changes rapidly due to higher biological activity, the autocorrelation function is expected to become narrower and results in a decrease in CL.

Plant and ozone exposure system

Chinese chives were grown in a growth chamber (CMP 3244, Conviron, Controlled Environmental Ltd, Canada.) maintaining at a relative humidity of 55% - 65% during 6.00 A.M. to 6.00 P.M. for the day shift and 6.00 P.M. to 6.00 A.M. for the night shift. Photon flux densities of 260 - 350 µmol m^{-2} s^{-1} and 0 µmol $m^{-2}s^{-1}$ and an air temperature of 25°C and 18°C were set for day and night shifts, respectively. The plants were kept regularly watered. In the experiment, healthy young leaves of the plants, one to two weeks old, were employed and mounted in a leaf O_3 chamber. Three halogen lamps

(PHL-150, MEJIRO PRECISION, Japan) with the fiber optic light guides were used to illuminate the plant leaf at a photon flux density of 500 µmol m^{-2} s^{-1} during the experiments.

The O_3 exposure system (Figure 3) consists of an air pump, charcoal filters (CF), an O_3 generator (OES 10A, Dylec Inc., Japan), an O_3 monitor (Model 1150, Dylec Inc., Japan), and a main O_3 chamber (33.5 × 33.5 × 58 cm^3). A specially designed leaf O_3 chamber (10 × 10 × 2 cm^3), made up of PVC was connected to the main O_3 chamber to enable optical imaging of the leaf. Generated O_3 was fed into the main O_3 chamber with its concentration being precisely controlled by the O_3 monitor that constantly sent a feedback signal to the O_3 generator. In the experiments, the O_3 generation system approximately took 14 minutes to reach the target O_3 concentration of 240 ppb. The O_3 feedback system practically stabilized the concentration of O_3 within the leaf and main O_3 chambers at an accuracy of 0.5% during the experiment.

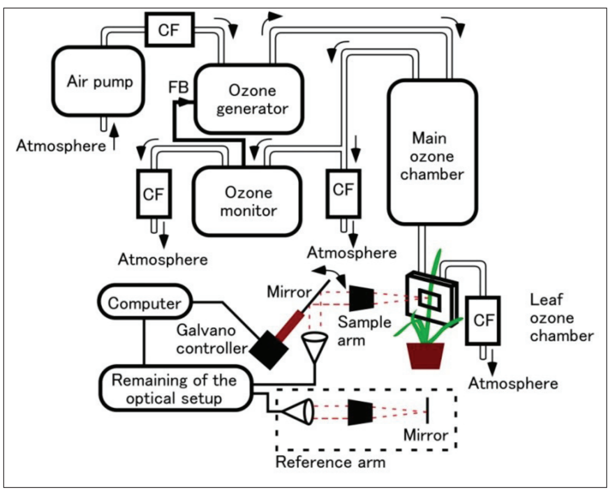

Figure 3: A schematic of the O_3 exposure system and a simplified sketch of SD-OCT system used in this study. CF: charcoal filter, FB: feed back signal. Arrows indicate the direction of air flow.

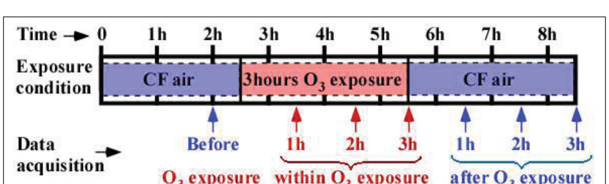

Figure 3: Timing protocol of O_3 exposure and data acquisition.

Timing protocol and data acquisition

Prior to the experiment, as an initial step, following mounting of the Chinese chives leaf in the leaf O_3 chamber, the leaf was acclimatized to the environmental condition by having a continuous flow of charcoal filtered air (10 liter/min.) into the leaf chamber for two hours. Next, after starting the O_3 generator half an hour was allocated for the O_3 concentration in the main O_3 chamber to reach 240 ppb. At the end of this half an hour period, on reaching the target O_3 concentration, connections of the O_3 air tubes were arranged in such a way that, air containing O_3 will reach leaf without passing through CF. O_3 exposure was carried out for 3 hours.

At the end of 3 hours of exposure, connection of O_3 tubes to the chamber were rearranged so as for the air to pass through CF before reaching the leaf chamber. Final CF air treatment was done to monitor the response of leaf after O_3 exposure. O_3 concentration of 240 ppb was chosen based on the criterion used in Japan, where serious warning for O_3 is issued (Lee & Goto, 2022; Rathnayake *et al.*, 2007). Both the temperature and the humidity were kept constant during a single session of the experiment with their variations being ± 2%.

bOCT biospeckle signal data corresponding to fixed lateral positions from the back surface of the leaf were acquired continuously at times including before O_3 exposure, during exposure at times of 1 hour, 2 hours, 3 hours, and after stopping O_3 exposure at 1 hour, 2 hours, and 3 hours. Before and after O_3 exposure, plant leaves were treated with CF air for 2.5 hours and 3 hours, respectively. The entire experimental duration was 8.5 hours.

Analyzing the biospeckle signals

To examine the bOCT biospeckles, OCT cross-sectional images were acquired successively over a certain period. Two different methods were used to analyze biospeckle signals coming from different spatial positions of the OCT cross-sectional image. In the first method, the magnitude of the fluctuation of the biospeckle signal, in other words, the standard deviation (SD) of the signal, was calculated along the time axis for each spatial position from the data array of OCT cross-sectional images. Then, a bOCT biospeckle image was constructed from the SDs of biospeckle signals.

In the second method, temporal characteristics of the biospeckle signals originating from different depths were analyzed. Averaged autocorrelation functions of bOCT biospeckle signals coming from layers at different depths of the leaf were calculated. From the correlation, half-width half maximum (HWHM) or the correlation length (CLs) was obtained. Longer CLs would indicate slower motion within the leaf and vice versa. Magnitude, SD, and temporal characteristics, CL, of the time varying biospeckle signal can reveal different information from that obtained by the conventional OCT, and they are proposed as measures to evaluate the changes in biological activities against O_3 stress on plants.

RESULTS AND DISCUSSION

Micro-structural cross-sectional observation with an optical microscope was done for a Chinese chives leaf (Figure 4). The epidermal cells layer indicated as *ue* (20 µm thick layer), and the oval shaped mesophyll cells marked as *mc* (around 90 µm in height), were clearly visible. Here, the epidermal layer is the outermost cell layer of the plant leaf, which regulates gas exchange, and protects the leaf against water loss. The mesophyll cell layer is the primary location for photosynthesis, governing most of the leaf's interior functions (Taiz & Zeiger, 2002).

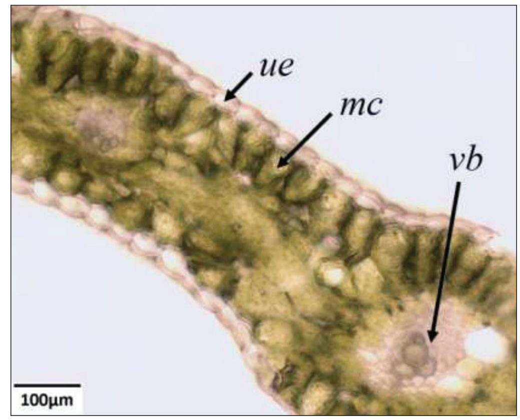

Figure 4: Optical microscopy (SZX7 Microscopy, U-TV0.5XC-3 Camera adaptor, OLYMPUS, Tokyo, Japan) analysis of the cross-section of a leaf of Chinese chives. ue-upper epidemis, mc-mesophyll cell, vb-vascular bundle.

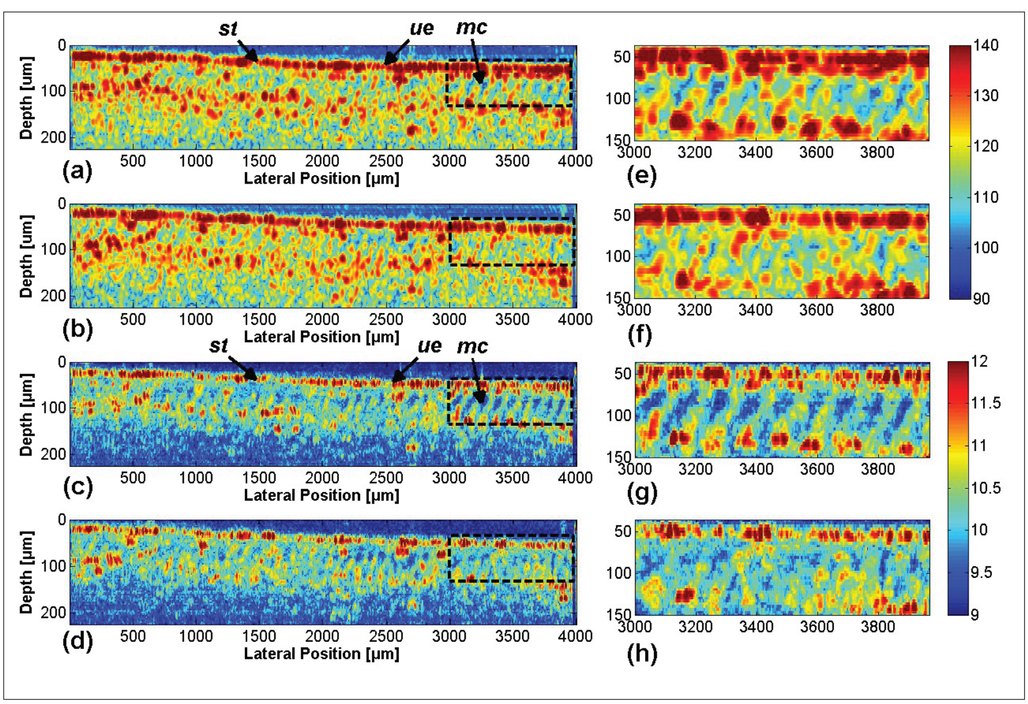

Figure 5: Conventional structural OCT cross-sectional images (a) before O_3 exposure, (b) 3 hours after starting O_3 exposure. Corresponding bOCT biospeckle images (c) before exposure, (d) 3 hours after starting O_3 exposure. Magnified views of the mesophyll cell layer encased in black dotted squares shown in (a), (b), (c), and (d) are shown, respectively in (e), (f), (g), and (h). ue: upper epidemis, mc: mesophyll cell.

Figures 5(a), and (b) show the conventional structural OCT image of Chinese chives leaf (abaxial surface) acquired before and 3 hours after starting O_3 exposure, respectively. Figures 5(c) and (d) represent the corresponding bOCT biospeckle SD images before, and 3 hours after starting O_3 exposure. The conventional OCT cross-sectional imaging can visualize the internal structure of biological tissues (Figure 5(a)). The epidermal cell layer can be clearly seen. However, the mesophyll cell layer was not clearly visible. In contrast, in the corresponding bOCT biospeckle image (Figure 5(c)), the layer structure becomes clearer, and it can be seen clearly in the magnified image shown in Figure 5(g) in comparison to the corresponding one in Figure 5(e) of the structural OCT image. Comparing with the microscopic image in Figure 3, the upper epidermal layer and the distinctive more oval shaped mesophyll cells can be clearly seen in the bOCT biospeckle image.

Comparing the effect of O_3 exposure duration, it was difficult to find a clear difference in conventional OCT images between Figures 5(a) and (b) or between (e), and (f). However, the variation due to O_3 exposure could be clearly seen in the bOCT biospeckle images between Figures 5(c) and (d), or (g) and (h). The oval shaped periodic structure that corresponds to mesophyll cells became unclear in biospeckle images with even 3 hours short term O_3 exposure. Earlier studies confirmed that cells belonging to mesophyll layer is the main target of O_3 injury (Turc *et al.*, 2023; Xu *et al.*, 2023; Vollenweider *et al.*, 2003). Next, biospeckle signals coming from different depth layers were analyzed for their temporal characteristics.

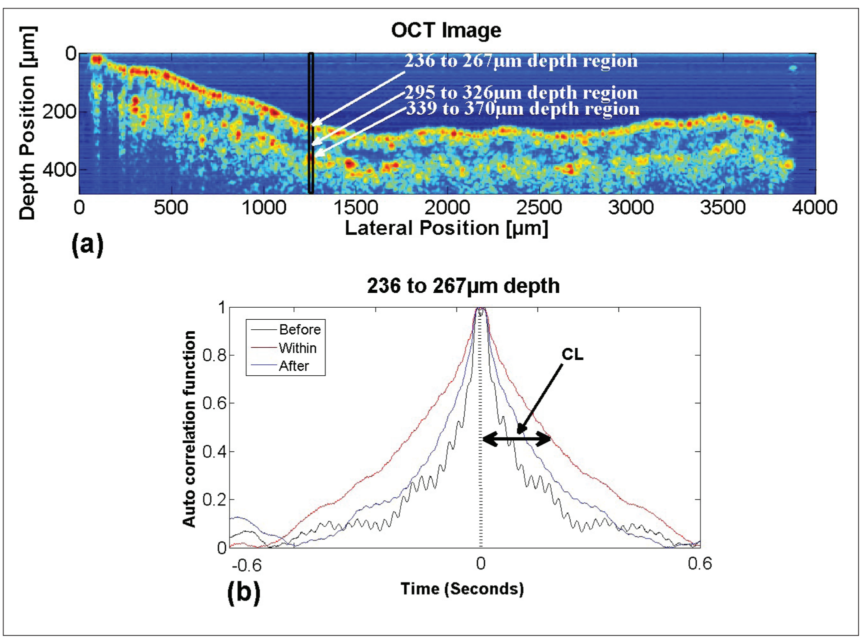

Figure 6: (a) OCT Image of the back surface of a leaf. (b) Averaged autocorrelation functions calculated for the epidermal layer over a region of 236 to 267µm across the depth.

It is clear from the origin of the biospeckles that in addition to its magnitude, SD, its temporal characteristics also reflect the dynamic properties of the cell organelles and scattering particles inside the plant leaf. To analyze the temporal characteristics of the signal, we examined the temporal autocorrelation function of the biospeckle signal.

In order to investigate the temporal autocorrelation function, the galvano mirrors used for scanning the beam laterally were fixed at a particular position of interest after the OCT images of the leaf were acquired (Figure 6(a)). Interference signals were acquired and the temporal autocorrelation functions corresponding to every depth position were calculated. The selected depth regions were the 236 to 267 μm depth region (epidermal layer), 295 to 326 μm depth region (mesophyll cell layer), and 339 to 370 μm depth region (layer below mesophyll cells). Autocorrelation functions within the same layer were averaged (along depth direction). The autocorrelation functions for different layers over different time periods of 1, 2, and 3 hours within the O_3 exposure duration were averaged and indicated as 'within'. In a similar way, autocorrelation functions for 1, 2, and 3 hours after exposure were averaged and indicated as 'after'.

Next, those autocorrelation functions were evaluated by defining the correlation length as half-width at half maximum, *i.e.*, CLs of biospeckle signals, and they were calculated for 'before', 'within', and 'after' O_3 exposure periods for each of the three different layers, namely, the *ue* layer, *mc* layer, and below *mc* layer.

The variation of CL under O_3 stress is shown in Figure 6(b) for the *ue* layer. It can be seen that CL increased with O_3 exposure, indicating that the rate of biological movements in this layer decreased with O_3 exposure in this layer. To focus on the relative change in biospeckle signal coming from three different layers of the leaf in response to O_3 exposure, CLs of biospeckle signals, those of 'within' and 'after' O_3 exposure were normalized using those obtained before O_3 exposure. These quantities are called as normalized correlation lengths (NCLs). NCLs from 16 measurements from the back surface of six different leaves (at least 2 measurements from one leaf) of Chinese chives, before, within, and after exposure to O_3 were averaged separately to obtain the averaged normalized correlation length (ANCL) as given by,

$$ANCL = \left\langle \frac{CL}{CL_b} \right\rangle, \quad \text{...(4)}$$

where, ‹...› denotes average over 16 measurements, and CL_b indicates the correlation length of the biospeckle signal before O_3 exposure. In the following discussion, the NCLs of biospeckle signals were used and shown for different layers in Figure 7. Under the short term of O_3 exposure, biological changes in different layers could be identified with ANCL.

ANCLs decreased in the *mc* layer and the below *mc* layer with O_3 exposure for the leaf. The reduction was significant (t-test, $P < 0.05$, Figure 7) in the case of the *mc* layer. However, for the *ue* layer ANCL appeared to be increased, but the increase was not statistically significant.

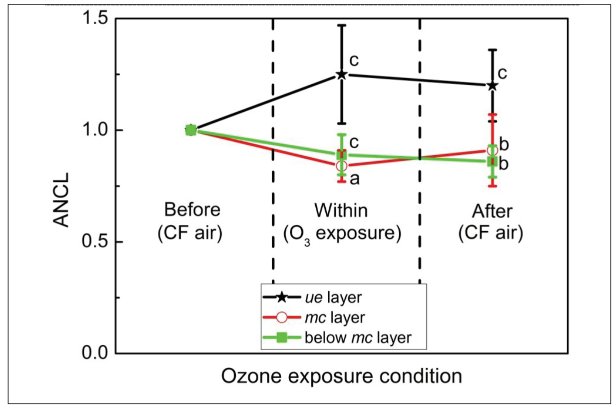

Figure 7: ANCLs of biospeckle signals coming from different layers (from the back surface) of Chinese chives leaves under O_3 exposures of 240 ppb. Each average value was plotted with standard error for 16 measurements. ue: upper epidemis, mc: mesophyll cell. The ANCL within O_3 exposure and after exposure were compared with that before exposure using statistical two samples t-test. (a, $P < 0.05$; b, $P < 0.07$; c, not significant).

Increase of CL, *i.e.*, slow fluctuation rate of the biospeckle signal, in the *ue* layer could be seen during and after the O_3 exposure. In contrast, the biospeckle fluctuation rate was increased during and even after O_3 exposure in the *mc* layer and the layer below mesophyll cells.

Earlier studies (Turc *et al.*, 2023; Xu *et al.*, 2023; Vollenweider *et al.* 2003; Faoro & Iriti 2009) too confirmed that palisade mesophyll cells are the main target of O_3 injury. Also, that the O_3 injury mainly occurs in the mesophyll cells whereas epidermal and stomatal cells and vascular cells resist until the last stage before total leaf necrosis. O_3 is taken up through the stomata and reacts with water and intercellular components to generate highly reactive oxygen species (ROS), that include peroxides and free radicals which are probably the real cause of the negative effect of O_3. Plants have a number of mechanisms that chemically and enzymatically remove these toxic compounds avoiding cellular damage (Kangasjärvi *et al.*, 1994, Sharma & Davis, 1997, Sandermann *et al.*, 1998, Dizengremel, 2001; Rajput *et al.*, 2021; Sachdev *et al.*, 2021). We expect that, once O_3 enters plant leaves, it activates these defense mechanisms. This may be a reason for the increase in biospeckle fluctuation rate in the *mc* layer and the layer below *mc*.

CONCLUSION

We showed that the bOCT biospeckle imaging technique can be successfully applied to monitor O_3 stress on plants. The internal cell structure of the leaf, especially the mesophyll cell layer and below, inside the Chinese chives leaf could be clearly visualized by the bOCT biospeckle imaging in contrast to the conventional OCT imaging. Further, with O_3 exposure, variation of magnitude of biospeckle signal fluctuation coming from mesophyll cell layer could be visualized with more of the oval shaped mesophyll cells becoming unclear in contrast to the conventional OCT image.

We showed that analysis of the temporal characteristics of biospeckle signal coming from different layers could identify changes in biological activity with O_3 exposure. This study demonstrates that the direct exposure to O_3 affects differently the bOCT biospeckle signals coming from different layers of Chinese chives, even though the period of exposure O_3 is short, only a few hours.

The bOCT based on biospeckle is found to be suitable for fast, non-destructive monitoring of environmental stresses on plants, which can potentially lead to significant time and cost saving, while conventional techniques require destruction and subsequent analysis.

Acknowledgement

This work was partly supported by the Grant-in-Aid for Science Research in JSPS (No. 24651023) of the Ministry of Education, Culture, Sports, Science and Technology in Japan.

REFERENCES

Ainsworth, E. A. (2008). Rice production in a changing climate: a meta-analysis of responses to elevated carbon dioxide and elevated ozone concentration. *Global Change Biology*, *14*(7), 1642-1650. https://doi.org/10.1111/j.1365-2486.2008.01594.x

Aizu, Y., & Asakura, T. (1996). Bio-speckles. *Trends in Optics*, 27-49. https://doi.org/10.1016/B978-012186030-1/50004-7

Ansari, M. Z., & Nirala, A. K. (2013). Biospeckle activity measurement of Indian fruits using the methods of cross-correlation and inertia moments. *Optik*, *124*(15), 2180-2186. https://doi.org/10.1016/j.ijleo.2012.06.081

Ashmore, M. R. (2005). Assessing the future global impacts of ozone on vegetation. *Plant, Cell and Environment*, *28*(8), 949-964. https://doi.org/10.1111/j.1365-3040.2005.01341.x

Baum, O. I., Zaitsev, V. Y., Yuzhakov, A. V., Sviridov, A. P., Novikova, M. L., Matveyev, A. L., Matveev, L. A., Sovetsky, A. A., & Sobol, E. N. (2020). Interplay of temperature, thermal-stresses and strains in laser-assisted modification of collagenous tissues: Speckle-contrast and OCT-based studies. *Journal of Biophotonics*, *13*(1), e201900199. https://doi.org/10.1002/jbio.201900199

Beig, G., Gunthe, S., & Jadhav, D. B. (2007). Simultaneous measurements of ozone and its precursors on a diurnal scale at a semi urban site in India. *Journal of Atmospheric Chemistry*, *57*, 239-253. https://doi.org/10.1007/s10874-007-9068-8

Beiu, R. M., Duma, V. F., Mnerie, C. A., Beiu, A. C., Dochia, M. A., Copolovici, L., Dobre, G., Bradu, A., & Podoleanu, A. (2022). *Optical coherence tomography versus microscopy for the study of Aloe vera leaves*. *Optics, Photonics and Digital Technologies for Imaging Applications*. SPIE.

Boccara, M., Schwartz, W., Guiot, E., Vidal, G., Paepe, R. D., Dubois, A., & Boccara, A. C. (2007). Early chloroplastic alterations analysed by optical coherence tomography during a harpin-induced hypersensitive response. *The Plant Journal*, *50*(2), 338-346. https://doi.org/10.1111/j.1365-313X.2007.03051.x

Bouma, B. E., de Boer, J. F., Huang, D., Jang, I. K., Yonetsu, T., Leggett, C. L., Leitgeb, R., Sampson, D. D., Suter, M., Vakoc, B. J., Villiger, M., & Wojtkowski, M. (2022). Optical coherence tomography. *Nature Reviews Methods Primers*, *2*(1), 79. https://doi.org/10.1038/s43586-022-00162-2

Braga Jr, R. A., Rabelo, G. F., Granato, L. R., Santos, E. F., Machado, J. C., Arizaga, R., ... & Trivi, M. (2005). Detection of fungi in beans by the laser biospeckle technique. *Biosystems Engineering*, *91*(4), 465-469. https://doi.org/10.1016/j.biosystemseng.2005.05.006

Braga, R. A., Dal Fabbro, I. M., Borem, F. M., Rabelo, G., Arizaga, R., Rabal, H. J., & Trivi, M. (2003). Assessment of seed viability by laser speckle techniques. *Biosystems Engineering*, *86*(3), 287-294. https://doi.org/10.1016/j.biosystemseng.2003.08.005

Braga, R. A., Dupuy, L., Pasqual, M., & Cardoso, R. R. (2009). Live biospeckle laser imaging of root tissues. *European Biophysics Journal*, *38*, 679-686. https://doi.org/10.1007/s00249-009-0426-0

Calatayud, A., Iglesias, D. J., Talón, M., & Barreno, E. (2003). Effects of 2-month ozone exposure in spinach leaves on photosynthesis, antioxidant systems and lipid peroxidation. *Plant Physiology and Biochemistry*, *41*(9), 839-845. https://doi.org/10.1016/S0981-9428(03)00123-2

Carvalho, P. H., Barreto, J. B., Braga Jr, R. A., & Rabelo, G. F. (2009). Motility parameters assessment of bovine frozen semen by biospeckle laser (BSL) system. *Biosystems Engineering*, *102*(1), 31-35. https://doi.org/10.1016/j.biosystemseng.2008.09.025

Chen, Y., Aguirre, A. D., Ruvinskaya, L., Devor, A., Boas, D. A., & Fujimoto, J. G. (2009). Optical coherence tomography (OCT) reveals depth-resolved dynamics during functional brain activation. *Journal of Neuroscience Methods*, *178*(1), 162-173. https://doi.org/10.1016/j.jneumeth.2008.11.026

Darrall, N. M. (1989). The effect of air pollutants on physiological processes in plants. *Plant, Cell and Environment*, *12*(1), 1-30. https://doi.org/10.1111/j.1365-3040.1989.tb01913.x

De Silva, Y. S. K., Rajagopalan, U. M., & Kadono, H. (2023a). Effect of alumina nanoparticles on lentil seed germination using biospeckle optical coherence tomography. *Applied Sciences*, *13*(16), 9203. https://doi.org/10.3390/app13169203

De Silva, Y. S. K., Rajagopalan, U. M., Kadono, H. & Li, D. (2023b). The synergy of microplastics with the heavy metal zinc has resulted in reducing the toxic effects of zinc on lentil (*Lens culinaris*) seed germination and seedling growth. *Heliyon*, *9*(11), e21464–e21464. https://doi.org/10.1016/j.heliyon.2023.e21464

De Silva, Y. S. K., Rajagopalan, U. M., Kadono, H., & Li, D. (2021). Positive and negative phenotyping of increasing Zn concentrations by biospeckle optical coherence tomography in speedy monitoring on lentil (*Lens culinaris*) seed germination and seedling growth. *Plant Stress*, *2*, 100041–100041. https://doi.org/10.1016/j.stress.2021.100041

De Silva, Y. S. K., Rajagopalan, U. M., Li, D., & Kadono, H. (2022). Optical screening method to observe the biological activities of lentil (*Lens culinaris*) seeds quantitatively under the exposure of polyethylene microplastics (PEMPs) using ultrahigh accurate biospeckle optical coherence tomography. In *Tissue Optics and Photonics II* (P. 19). SPIE. https://doi.org/10.1117/12.2620176

De Wit, J., Tonn, S., Van den Ackerveken, G., & Kalkman, J. (2020). Quantification of plant morphology and leaf thickness with optical coherence tomography. *Applied Optics*, *59*(33), 10304-10311. https://doi.org/10.1364/AO.408384

DeSilva, K. T. K. M., Rajagopalan, U. M., & Kadono, H. (2017). Highly sensitive optical interferometric technique reveals stress-dependent instantaneous nanometric growth fluctuations of Chinese chive leaf under heavy metal stress. *Ecotoxicology and Environmental Safety*, *137*, 86-93. https://doi.org/10.1016/j.ecoenv.2016.11.020

Dizengremel, P. (2001). Effects of ozone on the carbon metabolism of forest trees. *Plant Physiology and Biochemistry*, *39*(9), 729-742. https://doi.org/10.1016/S0981-9428(01)01291-8

Drexler, W., Morgner, U., Ghanta, R. K., Kärtner, F. X., Schuman, J. S., & Fujimoto, J. G. (2001). Ultrahigh-resolution ophthalmic optical coherence tomography. *Nature Medicine*, *7*(4), 502-507. https://doi.org/10.1038/86589

Everett, M., Magazzeni, S., Schmoll, T., & Kempe, M. (2021). Optical coherence tomography: From technology to applications in ophthalmology. *Translational Biophotonics*, *3*(1), e202000012. https://doi.org/10.1002/tbio.202000012

Faoro, F., & Iriti, M. (2009). Plant cell death and cellular alterations induced by ozone: key studies in Mediterranean conditions. *Environmental Pollution*, *157*(5), 1470-1477. https://doi.org/10.1016/j.envpol.2008.09.026

Feng, Z., Agathokleous, E., Yue, X., Oksanen, E., Paoletti, E., Sase, H., Gandin, A., Koike, T., Calatayud, V., Yuan, X., Liu, X., De Marco, A., Jolivet, Y., Kontunen-Soppela, S., Hoshika, Y., Saji, H., Li, P., Li, Z., Watanabe, M., & Kobayashi, K. (2021). Emerging challenges of ozone impacts on Asian plants: actions are needed to protect ecosystem health. *Ecosystem Health and Sustainability*, *7*(1), 1911602. https://doi.org/10.1080/20964129.2021.1911602

Fercher, A. F. (1996). Optical coherence tomography. *Journal of Biomedical Optics*, *1*(2), 157-173. https://doi.org/10.1117/12.231361

Fercher, A. F. (2010). Optical coherence tomography – development, principles, applications. *Zeitschrift für Medizinische Physik*, *20*(4), 251-276. https://doi.org/10.1016/j.zemedi.2009.11.002

Fujii, H., Asakura, T., Nohira, K., Shintomi, Y., & Ohura, T. (1985). Blood flow observed by time-varying laser speckle. *Optics Letters*, *10*(3), 104-106. https://doi.org/10.1364/OL.10.000104

Fujimoto, J. G. (2003). Optical coherence tomography for ultrahigh resolution in vivo imaging. *Nature Biotechnology*, *21*(11), 1361-1367. https://doi.org/10.1038/nbt892

Fujimoto, J. G. D. W., & Drexler, W. (2008). Introduction to optical coherence tomography. In *Optical coherence tomography: Technology and applications* (pp. 1-45). Springer. https://doi.org/10.1007/978-3-540-77550-8_1

Ge, X., Chen, S., Chen, S., & Liu, L. (2021). High resolution optical coherence tomography. *Journal of Lightwave Technology*, *39*(12), 3824-3835. https://doi.org/10.1109/JLT.2021.3061606

Gladkova, N., Maslennikova, A., Balalaeva, I., Feldchtein, F., Kiseleva, E., Karabut, M., & Iksanov, R. (2008). Application of optical coherence tomography in the diagnosis of mucositis in patients with head and neck cancer during a course of radio (chemo) therapy. *Medical Laser Application*, *23*(4), 186-195. https://doi.org/10.1016/j.mla.2008.07.008

Hettinger, J. W., Mattozzi, M. D. L. P., Myers, W. R., Williams, M. E., Reeves, A., Parsons, R. L., Haskell, R.C., Petersen, D.C., Wang, R., & Medford, J. I. (2000). Optical coherence microscopy. A technology for rapid, *in vivo*, non-destructive visualization of plants and plant cells. *Plant Physiology*, *123*(1), 3-16. https://doi.org/10.1104/pp.123.1.3

Holder, A. J., & Hayes, F. (2022). Substantial yield reduction in sweet potato due to tropospheric ozone, the dose-response function. *Environmental Pollution*, *304*, 119209. https://doi.org/10.1016/j.envpol.2022.119209

Hope, J., Goodwin, M., & Vanholsbeeck, F. (2021). Optical coherence tomography imaging of evoked neural activity in sciatic nerve of rat. *Journal of Physics D: Applied Physics*, 54(33), 334002. https://doi.org/10.1088/1361-6463/ac021b

Huang, D., Swanson, E. A., Lin, C. P., Schuman, J. S., Stinson, W. G., Chang, W., Hee, M.R., Flotte, T., Gregory, K., Puliafito, C.A., & Fujimoto, J. G. (1991). Optical coherence tomography. *Science*, *254*(5035), 1178-1181. https://doi.org/10.1126/science.1957169

Jiménez-Montenegro, L., Lopez-Fernandez, M., & Gimenez, E. (2021). Worldwide research on the ozone influence in plants. *Agronomy*, *11*(8), 1504. https://doi.org/10.3390/agronomy11081504

Kangasjärvi, J., Talvinen, J., Utriainen, M., & Karjalainen, R. (1994). Plant defence systems induced by ozone. *Plant, Cell and Environment*, *17*(7), 783-794. https://doi.org/10.1111/j.1365-3040.1994.tb00173.x

Kashani, A. H., Asanad, S., Chan, J. W., Singer, M. B., Zhang, J., Sharifi, M., Khansari, M. M., Abdolahi, F., Shi, Y., Biffi, A., Chui, H., & Ringman, J. M. (2021). Past, present and future role of retinal imaging in neurodegenerative disease. *Progress in Retinal and Eye Research*, *83*, 100938. https://doi.org/10.1016/j.preteyeres.2020.100938

Khateeb, K., Bloch, J., Zhou, J., Rahimi, M., Griggs, D. J., Kharazia, V. N., Le, M. N., Wang, R. K., & Yazdan-Shahmorad, A. (2022). A versatile toolbox for studying cortical physiology in primates. *Cell Reports Methods*, *2*(3). https://doi.org/10.1016/j.crmeth.2022.100183

Kobayashi, K., & Kadono, H. (2010). Expansion of the dynamic range of statistical interferometry and its application to extremely short- to long-term plant growth monitoring. *Applied Optics*, *49*(32), 6333-6339. https://doi.org/10.1364/AO.49.006333

Kobayashi, K., & Okada, M. (1995). Effects of ozone on the light use of rice (*Oryza sativa* L.) plants. *Agriculture, Ecosystems and Environment*, *53*(1), 1-12. https://doi.org/10.1016/0167-8809(94)00560-2

Kobayashi, K., Okada, M., & Nouchi, I. (1995). Effects of ozone on dry matter partitioning and yield of Japanese cultivars of rice (*Oryza sativa* L.). *Agriculture, Ecosystems and Environment*, *53*(2), 109-122. https://doi.org/10.1016/0167-8809(94)00564-U

Kumar, P., Kuttippurath, J., von der Gathen, P., Petropavlovskikh, I., Johnson, B., McClure-Begley, A., Cristofanelli, P., Bonasoni, P., Barlasina, M. E., & Sánchez, R. (2021). The increasing surface ozone and tropospheric ozone in Antarctica and their possible drivers. *Environmental Science and Technology*, *55*(13), 8542-8553. https://doi.org/10.1021/acs.est.0c08491

Kurenda, A., Adamiak, A., & Zdunek, A. (2012). Temperature effect on apple biospeckle activity evaluated with different indices. *Postharvest Biology and Technology*, *67*, 118-123. https://doi.org/10.1016/j.postharvbio.2011.12.017

Lee, J. H., & Goto, E. (2022). Ozone control as a novel method to improve health-promoting bioactive compounds in red leaf lettuce (*Lactuca sativa* L.). *Frontiers in Plant Science*, 13, 1045239. https://doi.org/10.3389/fpls.2022.1045239

Lee, J., Wijesinghe, R. E., Jeon, D., Kim, P., Choung, Y. H., Jang, J. H., Jeon, M., & Kim, J. (2018). Clinical utility of intraoperative tympanomastoidectomy assessment using a surgical microscope integrated with an optical coherence tomography. *Scientific Reports*, *8*(1), 17432. https://doi.org/10.1038/s41598-018-35563-5

Li, D., Rajagopalan, U. M., De Silva, Y. S. K., Liu, F., & Kadono, H. (2021a). Biospeckle optical coherence tomography (BOCT) in the speedy assessment of the responses of the seeds of *Raphanus sativus* L.(Kaiware Daikon) to acid mine drainage (AMD). *Applied Sciences*, *12*(1), 355. https://doi.org/10.3390/app12010355

Li, D., Rajagopalan, U. M., Kadono, H., & De Silva, Y. S. K. (2022). Speedy evaluation of simulated Acid Mine Drainage (AMD) on Rice by a non-invasive technique. *Plant Stress*, *6*, 100113. https://doi.org/10.1016/j.stress.2022.100113

Li, M., Rivera, S., Franklin, D., Nowak, E., Hallett, I., Kolenderska, S., Urbańska, M., Vanholsbeeck, F., & East, A. (2021). Use of optical coherence tomography and light microscopy for characterisation of mechanical properties and cellular level responses of 'Centurion' blueberries during weight loss. *Journal of Food Engineering*, *303*, 110596. https://doi.org/10.1016/j.jfoodeng.2021.110596

Li, P., Ni, S., Zhang, L., Zeng, S., & Luo, Q. (2006). Imaging cerebral blood flow through the intact rat skull with temporal laser speckle imaging. *Optics Letters*, *31*(12), 1824-1826. https://doi.org/10.1364/OL.31.001824

Lichtenegger, A., Gesperger, J., Niederleithner, M., Ginner, L., Woehrer, A., Drexler, W., Baumann, B., Leitgeb, R. A., & Salas, M. (2020). Ex vivo Alzheimer's disease brain tissue investigation: a multiscale approach using 1060 nm swept source optical coherence tomography for a direct correlation to histology. *Neurophotonics*, *7*(3), 035004. https://doi.org/10.1117/1.NPh.7.3.035004

Micieli, J., Lo, C., & Vuong, L. (2021). Recent advances and future directions on the use of optical coherence tomography in neuro-ophthalmology. *Taiwan Journal of Ophthalmology*, *11*(1), 3. https://doi.org/10.4103/tjo.tjo_76_20

Maheswari, R. U., Takaoka, H., Homma, R., Kadono, H., & Tanifuji, M. (2002). Implementation of optical coherence tomography (OCT) in visualization of functional structures of cat visual cortex. *Optics Communications*, *202*(1-3), 47-54. https://doi.org/10.1016/S0030-4018(02)01079-9

Maheswari, R. U., Takaoka, H., Kadono, H., Homma, R., & Tanifuji, M. (2003). Novel functional imaging technique from brain surface with optical coherence tomography enabling visualization of depth resolved functional structure *in vivo*. *Journal of Neuroscience Methods*, *124*(1), 83-92. https://doi.org/10.1016/S0165-0270(02)00370-9

Mariampillai, A., Leung, M. K., Jarvi, M., Standish, B. A., Lee, K., Wilson, B. C., Vitkin, A., & Yang, V. X. (2010). Optimized speckle variance OCT imaging of microvasculature. *Optics Letters*, *35*(8), 1257-1259. https://doi.org/10.1364/OL.35.001257

Mariampillai, A., Standish, B. A., Moriyama, E. H., Khurana, M., Munce, N. R., Leung, M. K., Jiang, J., Cable, A., Wilson, B.C., Vitkin, I.A., & Yang, V. X. (2008). Speckle variance detection of microvasculature using swept-source optical coherence tomography. *Optics Letters*, *33*(13), 1530-1532. https://doi.org/10.1364/OL.33.001530

Mathur, J. (2020). Morphology, behaviour and interactions of organelles. *Plant Science*, *301*, 110662. https://doi.org/10.1016/j.plantsci.2020.110662

Moayed, A. A., Hariri, S., Choh, V., & Bizheva, K. (2011). *In vivo* imaging of intrinsic optical signals in chicken retina with functional optical coherence tomography. *Optics Letters*, *36*(23), 4575-4577. https://doi.org/10.1364/OL.36.004575

Mogre, S. S., Brown, A. I., & Koslover, E. F. (2020). Getting around the cell: physical transport in the intracellular world. *Physical Biology*, 17(6), 061003. https://doi.org/10.1088/1478-3975/aba5e5

Pajuelo, M., Baldwin, G., Rabal, H., Cap, N., Arizaga, R., & Trivi, M. (2003). Bio-speckle assessment of bruising in fruits. *Optics and Lasers in Engineering*, *40*(1-2), 13-24. https://doi.org/10.1016/S0143-8166(02)00063-5

Pandiselvam, R., Mayookha, V. P., Kothakota, A., Ramesh, S. V., Thirumdas, R., & Juvvi, P. (2020). Biospeckle laser technique – A novel non-destructive approach for food quality and safety detection. *Trends in Food Science and Technology*, *97*, 1-13. https://doi.org/10.1016/j.tifs.2019.12.028

Panebianco, F., Rubiola, S., & Di Ciccio, P. A. (2022). The use of ozone as an eco-friendly strategy against microbial biofilm in dairy manufacturing plants: a review. *Microorganisms*, *10*(1), 162. https://doi.org/10.3390/microorganisms10010162

Pircher, M., Hitzenberger, C. K., & Schmidt-Erfurth, U. (2011). Polarization sensitive optical coherence tomography in the human eye. *Progress in Retinal and Eye Research*, *30*(6), 431-451. https://doi.org/10.1016/j.preteyeres.2011.06.003

Rajagopalan, U. M., Kabir, M., Lim, Y., & Kadono, H. (2020). Biospeckle optical coherence tomography in speedy visualizing effects of foliar application of plant growth hormone to Chinese chives leaves. *BMC Research Notes*, *13*, 1-6. https://doi.org/10.1186/s13104-020-05219-7

Rajput, V. D., Harish, Singh, R. K., Verma, K. K., Sharma, L., Quiroz-Figueroa, F. R., ... & Mandzhieva, S. (2021). Recent developments in enzymatic antioxidant defence mechanism in plants with special reference to abiotic stress. *Biology*, *10*(4), 267. https://doi.org/10.3390/biology10040267

Rathnayake, A. P., Kadono, H., Toyooka, S., & Miwa, M. (2007). Statistical interferometric investigation of nano-scale root growth: effects of short-term ozone exposure on ectomycorrhizal pine (*Pinus densiflora*) seedlings. *Journal of Forest Research*, *12*, 393-402. https://doi.org/10.1007/s10310-007-0040-x

Rathnayake, A. P., Kadono, H., Toyooka, S., & Miwa, M. (2008). A novel optical interference technique to measure minute root elongations of Japanese red pine (*Pinus densiflora* Seibold & Zucc.) seedlings infected with ectomycorrhizal fungi. *Environmental and Experimental Botany*, *64*(3), 314-321. https://doi.org/10.1016/j.envexpbot.2008.02.007

Ravichandran, N. K., Wijesinghe, R. E., Lee, S. Y., Choi, K. S., Jeon, M., Jung, H. Y., & Kim, J. (2017). Non-destructive analysis of the internal anatomical structures of mosquito specimens using optical coherence tomography. *Sensors*, *17*(8), 1897. https://doi.org/10.3390/s17081897

Ravichandran, N. K., Wijesinghe, R. E., Shirazi, M. F., Park, K., Lee, S. Y., Jung, H. Y., Jeon, M., & Kim, J. (2016). *In vivo* monitoring on growth and spread of gray leaf spot disease in *Capsicum annuum* leaf using spectral domain optical coherence tomography. *Journal of Spectroscopy*, *2016*(1), 1093734. https://doi.org/10.1155/2016/1093734

Reeves, A., Parsons, R. L., Hettinger, J. W., & Medford, J. I. (2002). *In vivo* three-dimensional imaging of plants with optical coherence microscopy. *Journal of Microscopy*, *208*(3), 177-189. https://doi.org/10.1046/j.1365-2818.2002.01086.x

Regar, E., van Leeuwen, A. M. G. J., & Serruys, P. W. (Eds.). (2007). *Optical coherence tomography in cardiovascular research*. CRC Press. https://doi.org/10.3109/9780203931561

Sachdev, S., Ansari, S. A., Ansari, M. I., Fujita, M., & Hasanuzzaman, M. (2021). Abiotic stress and reactive oxygen species: Generation, signaling, and defense mechanisms. *Antioxidants*, *10*(2), 277. https://doi.org/10.3390/antiox10020277

Saleah, S. A., Kim, S., Luna, J. A., Wijesinghe, R. E., Seong, D., Han, S., Kim, J., & Jeon, M. (2023). Optical coherence tomography as a non-invasive tool for plant material characterization in agriculture: A review. *Sensors*, *24*(1), 219. https://doi.org/10.3390/s24010219

Saleah, S. A., Lee, S. Y., Wijesinghe, R. E., Lee, J., Seong, D., Ravichandran, N. K., Jung, H. Y., Jeon M., & Kim, J. (2022). Optical signal intensity incorporated rice seed cultivar classification using optical coherence tomography. *Computers and Electronics in Agriculture*, *198*, 107014. https://doi.org/10.1016/j.compag.2022.107014

Saleah, S. A., Seong, D., Han, S., Wijesinghe, R. E., Ravichandran, N. K., Jeon, M., & Kim, J. (2021). Integrated quad-scanner strategy-based optical coherence tomography for the whole-directional volumetric imaging of a sample. *Sensors*, *21*(4), 1305. https://doi.org/10.3390/s21041305

Sandermann, H., Ernst, D., Heller, W., & Langebartels, C. (1998). Ozone: an abiotic elicitor of plant defence reactions. *Trends in Plant Science*, *3*(2), 47-50. https://doi.org/10.1016/S1360-1385(97)01162-X

Santiago, J. V., Inoue, K., & Tonokura, K. (2022). Modeling ground ozone concentration changes after variations in precursor emissions and assessing their benefits in the Kanto Region of Japan. *Atmosphere*, *13*(8), 1187. https://doi.org/10.3390/atmos13081187

Sharma, Y. K., & Davis, K. R. (1997). The effects of ozone on antioxidant responses in plants. *Free Radical Biology and Medicine*, *23*(3), 480-488. https://doi.org/10.1016/S0891-5849(97)00108-1

Silva, V. B., Andrade De Jesus, D., Klein, S., van Walsum, T., Cardoso, J., Brea, L. S., & Vaz, P. G. (2022). Signal-carrying speckle in optical coherence tomography: a methodological review on biomedical applications. *Journal of Biomedical Optics*, *27*(3), 030901-030901. https://doi.org/10.1117/1.JBO.27.3.030901

Singh, P., Chatterjee, A., Rajput, L. S., Rana, S., Kumar, S., Nataraj, V., Bhatia, V., & Prakash, S. (2021). Development of an intelligent laser biospeckle system for early detection and classification of soybean seeds infected with seed-borne fungal pathogen (*Colletotrichum truncatum*). *Biosystems*

Engineering, *212*, 442-457. https://doi.org/10.1016/j.biosystemseng.2021.11.002

Srimal, L. K. T. (2015a). *Development of functional optical coherence tomography (fOCT) for monitoring environmental effects on plants* (Doctoral dissertation, Saitama University, Saitama, Japan).

Srimal, L. K. T., Kadono, H., & Rajagopalan, U. M. (2013). Optical coherence tomography biospeckle imaging for fast monitoring varying surface responses of a plant leaf under ozone stress. *Proceedings of SPIE, the International Society for Optical Engineering*. https://doi.org/10.1117/12.2031062.

Srimal, L. K. T., Rajagopalan, U. M., & Kadono H. (2014). Optical Coherence Tomography (OCT) biospeckle signal analysis to investigate response of plant leaves to ozone. *Proceedings of the 23rd Congress of International Commission for Optics (ICO23), Santiago de Compostela, Spain.*

Srimal, L. K. T., Rajagopalan, U. M., & Kadono, H. (2015b). Functional optical coherence tomography (fOCT) biospeckle imaging to investigate response of plant leaves to ultra-short term exposure of Ozone. *Journal of Physics Conference Series*, *605*, 012013–012013. https://doi.org/10.1088/1742-6596/605/1/012013.

Srinivasan, V. J., Chen, Y., Duker, J. S., & Fujimoto, J. G. (2009). *In vivo* functional imaging of intrinsic scattering changes in the human retina with high-speed ultrahigh resolution OCT. *Optics Express*, *17*(5), 3861-3877. https://doi.org/10.1364/OE.17.003861

Steiner, R., Kunzi-Rapp, K., & Scharffetter-Kochanek, K. (2003). Optical coherence tomography: clinical applications in dermatology. *Medical Laser Application*, *18*(3), 249-259. https://doi.org/10.1078/1615-1615-00107

Szkulmowski, M., Gorczynska, I., Szlag, D., Sylwestrzak, M., Kowalczyk, A., & Wojtkowski, M. (2012). Efficient reduction of speckle noise in Optical Coherence Tomography. *Optics Express*, *20*(2), 1337-1359. https://doi.org/10.1364/OE.20.001337

Taiz, L., & Zeiger, E. (2002). *Plant Physiology*. Sunderland, MA. *Sinauer Associates, Inc., Publishers*, *3*, 484. https://pmc.ncbi.nlm.nih.gov/articles/PMC4242361/

Tang, X., Zhong, P., Gao, Y., & Hu, H. (2021a). Numerical model for evaluating the speckle activity and characteristics of bone tissue under the biospeckle laser system. *Journal of Innovative Optical Health Sciences*, *14*(06), 2150020. https://doi.org/10.1142/S1793545821500206

Tang, X., Zhong, P., Li, Z., Gao, Y., & Hu, H. (2021b). Evaluation of biological speckle activity: Using variational mode decomposition. *Optik*, *243*, 167475. https://doi.org/10.1016/j.ijleo.2021.167475

Thilakarathne, B. L. S., Rajagopalan, U. M., Kadono, H., & Yonekura, T. (2014). An optical interferometric technique for assessing ozone induced damage and recovery under cumulative exposures for a Japanese rice cultivar. *Springer Plus*, *3*, 1-12. https://doi.org/10.1186/2193-1801-3-89

Thilakarathne, B. L. S., Rajagopalan, U. M., Kadono, H., & Yonekura, T. (2014). High speed and high precision optical interferometric technique to investigate instantaneous growth related changes of plant leaves. *Plant Biotechnology*, *31*(3), 195-205. https://doi.org/10.5511/plantbiotechnology.14.0331a

Turc, B., Jolivet, Y., Cabané, M., Schaub, M., & Vollenweider, P. (2023). Ante- and post-mortem cellular injury dynamics in hybrid poplar foliage as a function of phytotoxic O_3 dose. *Plos one*, 18(3), e0282006. https://doi.org/10.1371/journal.pone.0282006

Vollenweider, P., Ottiger, M., & Günthardt-Goerg, M. S. (2003). Validation of leaf ozone symptoms in natural vegetation using microscopical methods. *Environmental Pollution*, *124*(1), 101-118. https://doi.org/10.1016/S0269-7491(02)00412-8

Wang, T., Xue, L., Feng, Z., Dai, J., Zhang, Y., & Tan, Y. (2022). Ground-level ozone pollution in China: a synthesis of recent findings on influencing factors and impacts. *Environmental Research Letters*, *17*(6), 063003. https://doi.org/10.1088/1748-9326/ac69fe

Wang, X., Manning, W., Feng, Z., & Zhu, Y. (2007). Ground-level ozone in China: distribution and effects on crop yields. *Environmental Pollution*, *147*(2), 394-400. https://doi.org/10.1016/j.envpol.2006.05.006

Wei, J., Li, Z., Li, K., Dickerson, R. R., Pinker, R. T., Wang, J., Liu, X., Sun, L., Xue, W., & Cribb, M. (2022). Full-coverage mapping and spatiotemporal variations of ground-level ozone (O_3) pollution from 2013 to 2020 across China. *Remote Sensing of Environment*, *270*, 112775. https://doi.org/10.1016/j.rse.2021.112775

Wei, X., & Gu, B. (Eds.). (2021). *Optical imaging in human disease and biological research*. Singapore: Springer. https://doi.org/10.1007/978-981-15-7627-0

Wijesinghe, R. E., Lee, S. Y., Kim, P., Jung, H. Y., Jeon, M., & Kim, J. (2016a). Optical inspection and morphological analysis of *Diospyros kaki* plant leaves for the detection of circular leaf spot disease. *Sensors*, *16*(8), 1282. https://doi.org/10.3390/s16081282

Wijesinghe, R. E., Lee, S. Y., Kim, P., Jung, H. Y., Jeon, M., & Kim, J. (2017a). Optical sensing method to analyze germination rate of *Capsicum annum* seeds treated with growth-promoting chemical compounds using optical coherence tomography. *Journal of Biomedical Optics*, *22*(9), 091502-091502. https://doi.org/10.1117/1.JBO.22.9.091502

Wijesinghe, R. E., Lee, S. Y., Ravichandran, N. K., Han, S., Jeong, H., Han, Y., Jung, H. Y., Kim, P., Jeon, M., & Kim, J. (2017b). Optical coherence tomography-integrated, wearable (backpack-type), compact diagnostic imaging modality for *in situ* leaf quality assessment. *Applied Optics*, *56*(9), D108-D114. https://doi.org/10.1364/AO.56.00D108

Wijesinghe, R. E., Lee, S. Y., Ravichandran, N. K., Shirazi, M. F., Kim, P., Jung, H. Y., Jeon, M., & Kim, J. (2018). Biophotonic approach for the characterization of initial bitter-rot progression on apple specimens using optical coherence tomography assessments. *Scientific Reports*, *8*(1), 15816. https://doi.org/10.1038/s41598-018-

33791-3

Wijesinghe, R. E., Park, K., Kim, P., Oh, J., Kim, S. W., Kim, K., Beop-Min Kim, Mansik Jeon, & Kim, J. (2016b). Optically deviated focusing method based high-speed SD-OCT for *in vivo* retinal clinical applications. *Optical Review*, *23*, 307-315. https://doi.org/10.1007/s10043-015-0154-x

Wojtkowski, M., Leitgeb, R., Kowalczyk, A., Bajraszewski, T., & Fercher, A. F. (2002). *In vivo* human retinal imaging by Fourier domain optical coherence tomography. *Journal of Biomedical Optics*, *7*(3), 457-463. https://doi.org/10.1117/1.1482379

Xu, Y., Feng, Z., Peng, J., & Uddling, J. (2023). Variations in leaf anatomical characteristics drive the decrease of mesophyll conductance in poplar under elevated ozone. *Global Change Biology*, *29*(10), 2804-2823. https://doi.org/10.1111/gcb.16621

Yoshikado, H. (2023). Correlation between air temperature and surface ozone in their extreme ranges in the greater Tokyo region. *Asian Journal of Atmospheric Environment*, *17*(1), 9. https://doi.org/10.1007/s44273-023-00010-z

Zdunek, A., Adamiak, A., Pieczywek, P. M., & Kurenda, A. (2014). The biospeckle method for the investigation of agricultural crops: A review. *Optics and Lasers in Engineering*, *52*, 276-285. https://doi.org/10.1016/j.optlaseng.2013.06.017

Zheng, S., Bai, Y., Xu, Z., Liu, P., & Ni, G. (2021). Optical coherence tomography for three-dimensional imaging in the biomedical field: a review. *Frontiers in Physics*, *9*, 744346. https://doi.org/10.3389/fphy.2021.744346